Revista Mexicana de Física
ISSN: 0035-001X
rmf@ciencias.unam.mx
Sociedad Mexicana de Física A.C.
México

Montenegro, V.; Orszag, M.
Generation of entanglement in cavity QED
Revista Mexicana de Física, vol. 57, núm. 3, julio, 2011, pp. 91-98
Sociedad Mexicana de Física A.C.
Distrito Federal, México

Generation of entanglement in cavity QED

V. Montenegro and M. Orszag
Facultad de Física, Pontificia Universidad Católica de Chile,
Casilla 306, Santiago, Chile

Recibido el 20 de enero de 2011 ; aceptado el 9 de marzo de 2011

We present a model to generate atomic entanglement with atoms located at distant cavities. It consists of two cavities connected by an optical fiber, where each cavity interacts with a single two-level atom. For certain atom-cavity and cavity-fiber coupling parameters, we find a wide time plateau for the concurrence between the atoms. An increase of the atom-cavity detuning, gives rise to a linear increase of the width of the plateau, but at the same time, when losses are included in the model, it also decreases the value of the concurrence and increases the response time to reach the maximum.

Keywords: Entanglement; distant cavities; cavity QED; microscopic master equation.

Presentamos un modelo para generar entrelazamiento con átomos localizados en cavidades distantes. Consiste en dos cavidades conectadas por una fibra óptica, donde cada cavidad interactua con un solo átomo de dos niveles. Para ciertos valores de los parámetros de acoplamiento átomo–cavidad y cavidad–fibra, encontramos un $plateau$ amplio en el tiempo para la concurrencia entre los átomos. El aumento del desentonamiento átomo-cavidad da lugar a un aumento líneal en el ancho del $plateau$, pero al mismo tiempo, cuando las pérdidas son tomadas en cuenta en el modelo, el valor de la concurrencia decrece y aumenta el tiempo de respuesta necesario para alcanzar el máximo.

Descriptores: Entrelazamiento; cavidades distantes; electrodinámica cuántica de cavidades; ecuación maestra microscópica.

PACS: 03.65.-w; 03.65.Ud; 03.65.Yz

1. Introduction

Quantum entanglement has been understood as the basic and essential resource in quantum information and of paramount importance in a number of applications such as quantum cryptography and quantum teleportation. Also, many groups [1–5] have used these relevant quantum states to expose the limits and nature of quantum theory, for example in the frame of locality, realism and theoretical completeness [6].

The Jaynes-Cummings model (JCM) [7,8] in the rotating-wave approximations (RWA), is the fundamental model for the quantum description of matter-light interaction. It provides the general framework to describe the interaction of a two-level system, such as an atom, with a quantized cavity mode (normally termed cavity quantum electrodynamics (CQED)). This model appears as one of the key ingredients for applications in quantum information processing.

Using the JCM, many successful CQED experiments have been implemented with microwave cavities and Rydberg atoms in the strong coupling regime [9–13], *i.e.* when the coupling rate g exceeds the dissipation rates κ and γ of both, cavity and atom, giving rise to coherent light-matter oscillations and superposition states.

At present time, an important improvement in the lifetime of a photon in a microwave cavity [13] has been achieved, as compared to experiments performed more than ten years ago [11, 12].

Recently, several groups have studied various schemes of atomic entanglement, using for example, one atom in each cavity or two atoms in the same cavity [14–16].

Also, Pellizzari [17] proposed a new system composed of two remote cavities connected by an optical fiber. Some recent publications based on Pellizari's idea proposed examples such as: A scheme to generate multiparticle entanglement [18], also, the generation of an EPR pair of atoms interacting successively and simultaneously with the coupled cavities system [19], and using distant cavities coupled to an optical fiber and multiple two-level atoms trapped in the cavities, could be showed that there exist highly reliable quantum swap, entangling, and controlled-Z gates [20]. Finally, some recent papers studied steady state polariton entanglement in a pumped cavity QED system [21, 22].

The present work consists in two cavities connected by an optical fiber, where each cavity interacts with a single atom. We show that in the present system, we can generate a time plateau of entanglement, starting from a separable mixed state. Furthermore, this generated entanglement is robust to any perturbation of the initial state. This is the highest entanglement presented (with a concurrence between 0.99 and 1) during a long time plateau, spontaneously generated and without any pumps.

We study the dependence of the width of concurrence plateau with the atom-cavity detuning, and with various coupling constants and loss parameters. We also analyze the maximum concurrence, versus the atom-cavity detuning. We observe a linear increase of the width of the plateau with the detuning, but also, when losses are included in the model, a decrease in the maximum concurrence, as well as an increase of the response time of our system.

The paper is structured as follows. In Sec. 2 we give a full description of our model, as well as our notation. In Sec. 3 we present the microscopic master equation approach, in order to model the losses of the system in contact with an environment at zero temperature, using the Davies operators

that correspond to the quantum jumps between the dressed-states of the Hamiltonian of the system $\hat{H}_s$. In Sec. 4 we describe the dynamics of the entanglement by solving the microscopic master equation at zero temperature, including an initial mixed state with zero concurrence. We show that, in order to generate atomic entanglement, we need to measure the vacuum state for cavities an the optical fiber. In Sec. 5, we show the numerical results for the concurrence, and finally we present the conclusions in Sec. 6.

2. The model

We consider two two-level atoms interacting with two different cavities coupled by an optical fiber (Fig. 1).

The Hamiltonian ($\hbar = 1$) of the system in the RWA is:

$$\hat{H}_s = \omega_c \hat{a}_3^\dagger \hat{a}_3 + \sum_{j=1,2} [\omega_a \hat{S}_{j,z} + \omega_c \hat{a}_j^\dagger \hat{a}_j + g_j(\hat{a}_j \hat{S}_{j,+} + \hat{a}_j^\dagger \hat{S}_{j,-}) + \nu(\hat{a}_3 \hat{a}_j^\dagger + \hat{a}_3^\dagger \hat{a}_j)], \quad (1)$$

where $\hat{a}_3$ is the boson operator for the fiber, $\hat{a}_j$ are the cavity operators, and $\hat{S}_{j,z}, \hat{S}_\pm$ are the atomic operators. ω_c, ω_a are the fiber (cavity) and the atomic frequencies and g_j, ν the atom-cavity and cavity-fiber coupling constants.

In Eq. (1) we define the following operators,

$$\hat{S}_{j,z} = \frac{1}{2}\left(|e\rangle_{jj}\langle e| - |g\rangle_{jj}\langle g|\right),$$
$$\hat{S}_{j,+} = |e\rangle_{jj}\langle g|, \quad \hat{S}_{j,-} = |g\rangle_{jj}\langle e|.$$

Also, we have considered the short fiber limit in Eq. (1), *i.e.*, only one mode (resonant) of the fibre will interact with the cavity modes. We recall that the coupling ν to the modes of a fibre of finite length can be estimated as $\nu \simeq \sqrt{4\pi\bar{\nu}c/l}$, where l is the finite length of the optical fiber (for instance $l \lesssim 1$m), c is the speed of light in vacuum, and $\bar{\nu}$ corresponds to the decay rate of the cavities' fields into a continuum of fibre modes. Furthermore, the finite length of the fibre implies a quantization of the modes of the fibre with a frequency spacing given by $2\pi c/l$. Finally, from an experimental point of view, we can notice that the coupling strength ν can be increased by decreasing the reflectivity of the cavity mirror connected to the fibre [23].

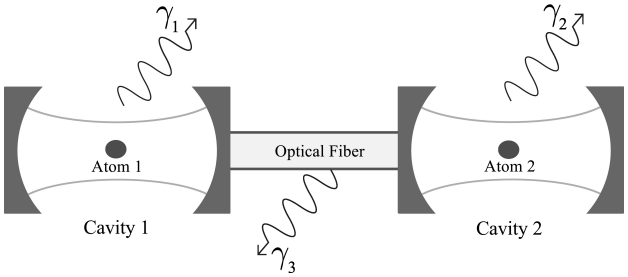

FIGURE 1. Two atoms interact with two distant cavities coupled by an optical fiber. In the figure γ_1, γ_2 and γ_3 correspond to damping constant for the cavities and optical fiber respectively.

In the present work we have used the following notation for the basis of the system

$$|i\rangle = |A_1\rangle \otimes |A_2\rangle \otimes |C_1\rangle \otimes |C_2\rangle \otimes |F\rangle = |A_1 A_2 C_1 C_2 F\rangle,$$

where $A_{j=1,2}$ correspond to the atomic states, that can be $e(g)$ for excited(ground) state, while $C_{j=1,2}$ are the cavities states, and F corresponds to the state of the optical fiber. Both $C_{j=1,2}$ and F can correspond to a 0 or 1 photon state. Also, we denote by $|\phi_k\rangle$ as the k-th dressed-state of the Hamiltonian $\hat{H}_s$ with eigenvalue λ_k, this eigenstate of $\hat{H}_s$ has all the atom and field information. Therefore, in the general case $|\phi_k\rangle$ will be a linear combination of the basis vectors described above.

In addition, we assume the system at zero temperature with a single excitation, with this assumptions we can constrain the Hilbert space only to five vectors with a single excitation, plus the ground state of the system without excitation. It is important indicate that, this restriction is valid only in the case at zero temperature, because the system cannot increases the number of excitations in the temporal evolution, and therefore at non-zero temperature the assumptions of having only six vectors on the Hilbert space is no longer valid.

Using the notation described previously, and considering the system at zero temperature, we have the following basis:

$$|1\rangle = |eg000\rangle, \quad |2\rangle = |gg100\rangle,$$
$$|3\rangle = |gg001\rangle, \quad |4\rangle = |gg010\rangle,$$
$$|5\rangle = |ge000\rangle, \quad |6\rangle = |gg000\rangle, \quad (2)$$

where, the vectors of the system $\{|1\rangle, \ldots, |5\rangle\}$ corresponds for one excitation, and the state $|6\rangle = |gg000\rangle$ has been included due to the system losses.

Using the above basis in Eq. (2), it is straightforward to show that we can write the Hamiltonian $\hat{H}_s$ in Eq. (1) in a matrix representation, as

$$\hat{H}_s = \begin{pmatrix} 0 & g_1 & 0 & 0 & 0 & 0 \\ g_1 & \Delta & \nu & 0 & 0 & 0 \\ 0 & \nu & 0 & \nu & 0 & 0 \\ 0 & 0 & \nu & \Delta & g_2 & 0 \\ 0 & 0 & 0 & g_2 & 0 & 0 \\ 0 & 0 & 0 & 0 & 0 & -\omega_a \end{pmatrix}, \quad (3)$$

where $\Delta = \omega_c - \omega_a$ is the atom-cavity detuning.

3. Microscopic master equation

In cavity quantum electrodynamics the main source of dissipation originates from the leakage of the cavity photons due to imperfect reflectivity of the cavity mirrors. A second source of dissipation corresponds to spontaneous emission of photons by the atom, however is mostly suppressed by the presence of the cavity, and therefore its effect is usually neglected.

In order to model the losses, we will use an approach called the microscopic master equation presented by Scala *et al.* [24,25], which goes back to the original ideas of Davies on how to describe the system-reservoir interactions in markovian master equations [26, 27]. This description considers jumps between eigenstates of the system Hamiltonian rather than the eigenstates of the field-free subsystems, which is the case in many approaches employed in quantum optics.

We assume that our system of interest, *i.e.*, atoms, cavities and the optical fiber, are part of a larger system, composed by a collection of quantum harmonic oscillators in thermal equilibrium at temperature T. This external environment is that part of the total closed system other than the system of interest. The evolution of the total closed system is governed by the Hamiltonian $\hat{H}$ given by,

$$\hat{H} = \hat{H}_s + \hat{H}_r + \hat{H}_{int},$$

where $\hat{H}_s$ corresponds to Eq. (1), and $\hat{H}_r$ is the Hamiltonian of the reservoir at temperature T written as

$$\hat{H}_r = \sum_{\substack{j=1 \\ i=\{1,2,3\}}}^{\infty} \omega_{ij} \hat{r}_{ij}^{\dagger} \hat{r}_{ij}. \tag{4}$$

In Eq. (4), ω_{ij} indicates the frequency related to the operator $\hat{r}_{ij}^{\dagger}\hat{r}_{ij}$ corresponding to the harmonic oscillators of the reservoirs. Both the frequencies and the harmonic oscillators are in the j-th mode of the cavities (i=1,2) or the fiber (i=3), finally, as we are interested in generate entanglement between distant cavities, we can establish that the cavities and the optical fiber have independent reservoirs.

The interaction Hamiltonian $\hat{H}_{\text{int}}$ is given by:

$$\hat{H}_{\text{int}} = \sum_{\substack{j=1 \\ i=\{1,2,3\}}}^{\infty} \Omega_{ij} \left(\hat{a}_i + \hat{a}_i^{\dagger} \right) \otimes \left(\hat{r}_{ij}^{\dagger} + \hat{r}_{ij} \right), \tag{5}$$

where Ω_{ij} corresponds to the interaction frequency between the cavities (and fiber) fields with the j-th mode of the reservoirs, also, we can note that the Eq. (5) has the following form,

$$\begin{aligned} \hat{H}_{int} &= \hat{A}_1 \otimes \hat{R}_1 + \hat{A}_2 \otimes \hat{R}_2 + \hat{A}_3 \otimes \hat{R}_3, \\ \hat{A}_1 &= \hat{a}_1 + \hat{a}_1^{\dagger}, \\ \hat{A}_2 &= \hat{a}_2 + \hat{a}_2^{\dagger}, \\ \hat{A}_3 &= \hat{a}_3 + \hat{a}_3^{\dagger}, \end{aligned} \tag{6}$$

where the $\hat{A}_j$ and $\hat{R}_j$ are operators acting on the system $\hat{H}_s$ and on the environmental Hilbert spaces, respectively.

Following the standard procedures [28], *i.e.*, writing down the Liouville-von Neumann equation for the total density operator in the interaction picture with respect to $\hat{H}_s + \hat{H}_r$, performing the Born-Markov and RWA, tracing out the environmental degrees of freedom and then going back to the Schrödinger picture, one obtains the microscopic master equation for the reduced density operator $\hat{\rho}(t)$ of the system. In our case, we have considered the system at zero-temperature, in this case the microscopic master equation at zero temperature has the following form:

$$\begin{aligned} \dot{\hat{\rho}}(t) = -i[\hat{H}_s, \hat{\rho}(t)] + \sum_{\substack{\bar{\omega}>0 \\ n=1,2,3}} \gamma_n(\bar{\omega}) [\hat{A}_n(\bar{\omega}) \hat{\rho}(t) \hat{A}_n^{\dagger}(\bar{\omega}) \\ - \frac{1}{2} \{ \hat{A}_n^{\dagger}(\bar{\omega}) \hat{A}_n(\bar{\omega}), \hat{\rho}(t) \}], \end{aligned} \tag{7}$$

where in Eq. (7), the first part (commutator) corresponds to a non-dissipative evolution, the second part includes the system losses. As we have mentioned before, $n = \{1, 2\}$, and $n = 3$ corresponds to the channels of dissipations for the cavities and the optical fiber (all independents) respectively. Furthermore, $\bar{\omega}$ corresponds to Bohr's frequencies (transitions between the eigenstates $|\phi_m\rangle$) related to $\hat{H}_s$, and $\gamma_n(\bar{\omega})$ is the damping parameter related to that transition. Also, these frequencies are positive due to transitions only downward in the energy ladder. Finally, the Davies operators [28] $\hat{A}_n(\bar{\omega})$ are quantum jumps between the dressed-states of $\hat{H}_s$, and correspond to the following expression:

$$\hat{A}_n(\bar{\omega}) = \sum_{\bar{\omega}=\lambda_\beta-\lambda_\alpha} |\phi_\alpha\rangle \langle\phi_\alpha| \hat{A}_n |\phi_\beta\rangle \langle\phi_\beta| ,$$

where, $|\phi_m\rangle$ is the m-th dressed-state of $\hat{H}_s$, this state has the information about the fields of the cavities and optical fiber, as well as the atomic information. As we can see, $\bar{\omega} = \lambda_\beta - \lambda_\alpha$ are the Bohr's frequencies between transitions $|\phi_\beta\rangle \longrightarrow |\phi_\alpha\rangle$, where in our case the eigenvalues related to this transition are: $\lambda_\beta > \lambda_\alpha$, due to that our system is at zero temperature and only are allowed transitions downward in the energy ladder.

4. Dynamics of entanglement

4.1. Formal solution of the microscopic master equation at zero temperature

In the most general case, we will have different coupling constants, small atom-cavity detuning, and dissipative factors. In this general case, there is not an analytic solution using the matrix representation showed in Eq. (3). For that reason, we have adopted a formal solution and at the end, we will make use of numerical analysis.

We assume that, for each eigenvalue λ_i, there will be a normalized dressed-state $|\phi_i\rangle$ acting on $\hat{H}_s$ (see Eq. (3)), of the following form:

$$\underbrace{\begin{pmatrix} |\phi_1\rangle \\ |\phi_2\rangle \\ |\phi_3\rangle \\ |\phi_4\rangle \\ |\phi_5\rangle \\ |\phi_6\rangle \end{pmatrix}}_{|\Phi\rangle} = \underbrace{\begin{pmatrix} c_1 & c_2 & c_3 & c_4 & c_5 & 0 \\ c_6 & c_7 & c_8 & c_9 & c_{10} & 0 \\ c_{11} & c_{12} & c_{13} & c_{14} & c_{15} & 0 \\ c_{16} & c_{17} & c_{18} & c_{19} & c_{20} & 0 \\ c_{21} & c_{22} & c_{23} & c_{24} & c_{25} & 0 \\ 0 & 0 & 0 & 0 & 0 & 1 \end{pmatrix}}_{C} \underbrace{\begin{pmatrix} |1\rangle \\ |2\rangle \\ |3\rangle \\ |4\rangle \\ |5\rangle \\ |6\rangle \end{pmatrix}}_{|J\rangle} \tag{8}$$

where, in Eq. (8), we have defined the vector of dressed-states by $|\Phi\rangle$, the vector of basis-states by $|J\rangle$, and finally, the matrix C that relates both.

On the other hand, $\{|\phi_1\rangle, \ldots, |\phi_5\rangle\}$, is the subspace in absence of losses. The single state $|\phi_6\rangle = |6\rangle = |gg000\rangle$, corresponds to the ground state of the full system.

With the formalism showed above, and according to the definition in Eq. (6), we can calculate the operators $\hat{A}_n(\bar{\omega})$, as follows:

$$\hat{A}_n(\bar{\omega}_{\alpha\beta}) = |\phi_\alpha\rangle \langle\phi_\alpha| \left(\hat{a}_n + \hat{a}_n^\dagger\right) |\phi_\beta\rangle \langle\phi_\beta|, \tag{9}$$

where, we have defined $\bar{\omega}_{\alpha\beta} = \lambda_\beta - \lambda_\alpha$. However, we are interested in the case of zero temperature, thus we use the fact that $\hat{a}_n^\dagger$ applied to any state corresponding to $\{|\phi_1\rangle, \ldots, |\phi_5\rangle\}$ is zero, because the number of excitations cannot increase in time. This assumption implies a convenient constraint on the Hilbert space. Indeed, at zero temperature the system can make transitions only downward on the energy ladder.

For that reason, the operators in Eq. (9), are reduced to:

$$\hat{A}_n(\bar{\omega}_{\alpha\beta}) = |\phi_\alpha\rangle \langle\phi_\alpha| \hat{a}_n |\phi_\beta\rangle \langle\phi_\beta|. \tag{10}$$

Once we have the operators $\hat{A}_n(\bar{\omega}_{\alpha\beta})$, it is straightforward to find the matrix elements of $\hat{\rho}(t)$ in Eq. (7). Also, we need to define the initial conditions (which we address in the next section), to solve the full set of first-order differential equations.

4.2. Initial condition to solve Microscopic Master Equation at zero temperature

We assume an initial state with a single atomic excitation and introduce a parameter α that varies the mixedness of the initial state. The initial condition can be written easily in the vector basis, however, the evolution of the system is written in the dressed-state basis. Therefore, we need to perform a change of basis

$$\hat{\rho}(0) = \sum_{i,j} \langle i| \hat{\rho}(0) |j\rangle |i\rangle \langle j| = \sum_{i,j} \langle\phi_i| \hat{\rho}(0) |\phi_j\rangle |\phi_i\rangle \langle\phi_j|.$$

In order to carry out the above conversion, we adopt a formal solution that will be computed numerically at the end.

Inverting Eq. (8), we get:

$$\underbrace{\begin{pmatrix} |1\rangle \\ |2\rangle \\ |3\rangle \\ |4\rangle \\ |5\rangle \\ |6\rangle \end{pmatrix}}_{|J\rangle} = \underbrace{\begin{pmatrix} \tilde{c}_1 & \tilde{c}_2 & \tilde{c}_3 & \tilde{c}_4 & \tilde{c}_5 & 0 \\ \tilde{c}_6 & \tilde{c}_7 & \tilde{c}_8 & \tilde{c}_9 & \tilde{c}_{10} & 0 \\ \tilde{c}_{11} & \tilde{c}_{12} & \tilde{c}_{13} & \tilde{c}_{14} & \tilde{c}_{15} & 0 \\ \tilde{c}_{16} & \tilde{c}_{17} & \tilde{c}_{18} & \tilde{c}_{19} & \tilde{c}_{20} & 0 \\ \tilde{c}_{21} & \tilde{c}_{22} & \tilde{c}_{23} & \tilde{c}_{24} & \tilde{c}_{25} & 0 \\ 0 & 0 & 0 & 0 & 0 & 1 \end{pmatrix}}_{C^{-1}=\tilde{C}} \underbrace{\begin{pmatrix} |\phi_1\rangle \\ |\phi_2\rangle \\ |\phi_3\rangle \\ |\phi_4\rangle \\ |\phi_5\rangle \\ |\phi_6\rangle \end{pmatrix}}_{|\Phi\rangle}. \tag{11}$$

In general, we consider the following initial condition:

$$\hat{\rho}(0) = \alpha |eg000\rangle \langle eg000| + (\alpha - 1) |ge000\rangle \langle ge000|, \tag{12}$$

where, the parameter $0 \leq \alpha \leq 1$, indicates how mixed our initial state is.

Using the Eqs. (11) and (12), we can write explicitly the initial condition in the dressed-states basis.

4.3. Generation of atomic entanglement: Measuring the vacuum state for the cavities and the optical fiber

At this point, we have the complete evolution of our system. However, in order to generate atomic entanglement, we need to perform a measurement on the cavities and fiber states.

To accomplish the measurement, we begin with the state:

$$\hat{\rho}(t) = \sum_{i,j=1}^{6} \langle\phi_i| \hat{\rho}(t) |\phi_j\rangle |\phi_i\rangle \langle\phi_j|, \tag{13}$$

where Eq. (13), represents the full evolution of our system with the elements $\langle\phi_i| \hat{\rho}(t) |\phi_j\rangle$.

Next, we project our solution onto the state

$$|000\rangle = |0\rangle_{C1} \otimes |0\rangle_{C2} \otimes |0\rangle_F,$$

and readily get:

$$\hat{\tilde{\rho}}(t) = \langle 000|\, \hat{\rho}(t)\, |000\rangle$$
$$= \sum_{i,j=1}^{6} \langle \phi_i|\, \hat{\rho}(t)\, |\phi_j\rangle \langle 000\, |\phi_i\rangle \langle \phi_j|\, 000\rangle, \qquad (14)$$

where, in Eq. (14) we define the non-normalized state $\hat{\tilde{\rho}}(t)$, that represents the state of the system after the measurement.

Using the Eqs. (2), (8) and (14), we observe that the elements of $\hat{\tilde{\rho}}(t)$ form a X-matrix. In the standard two-qubit product basis $\{|ee\rangle, |eg\rangle, |ge\rangle, |gg\rangle\}$, a X-matrix can be written as follows:

$$\hat{\varrho}(t) = \begin{pmatrix} \rho_{ee,ee} & 0 & 0 & \rho_{ee,gg} \\ 0 & \rho_{eg,eg} & \rho_{eg,ge} & 0 \\ 0 & \rho_{ge,eg} & \rho_{ge,ge} & 0 \\ \rho_{gg,ee} & 0 & 0 & \rho_{gg,gg} \end{pmatrix},$$

where we have used the notation $\rho_{ab,cd} = \langle ab|\, \hat{\rho}(t)\, |cd\rangle$ for the matrix elements, and

$$\rho_{ee,ee} + \rho_{eg,eg} + \rho_{ge,ge} + \rho_{gg,gg} = 1.$$

Furthermore, in our case, due to the election of the initial condition, and the constrain of the Hilbert space for a single excitation, the elements with two excitations $\rho_{ee,ee}, \rho_{ee,gg}$ and $\rho_{gg,ee}$ are not present in our description. Therefore, due to the statistical mixture and the presence of losses in the system we get a X-matrix only with the following non-zero elements $\rho_{eg,eg}, \rho_{eg,ge}, \rho_{ge,eg}, \rho_{gg,gg}$ and $\rho_{ge,ge}$, where we can easily compute the concurrence [29, 30] as follows:

$$C(t) = 2\left|\frac{\rho_{eg,ge}}{\rho_{eg,eg} + \rho_{ge,ge} + \rho_{gg,gg}}\right|.$$

5. Numerical results

As we have described in the previous sections, in order to model the leakage of cavity photons, and also the losses in the optical fiber, we need to specify the decay parameter $\gamma_n(\bar{\omega})$. These coefficients are given by the Fourier transform of the correlation functions of the environment [25, 28].

$$\gamma(\bar{\omega}) = \int_{-\infty}^{\infty} d\tau \mathrm{e}^{i\bar{\omega}\tau} \langle \hat{E}^{\dagger}(\tau)\hat{E}(0)\rangle, \qquad (15)$$

where the environment operators $\hat{E}$ are in the interaction picture.

However, in our analysis, the damping parameters correspond to $\gamma_n(\omega_a + \lambda_i)$, where ω_a is the transition frequency of the atom, and λ_i are the Bohr frequencies relative to $\hat{H}_s$. Furthermore, since in our case $\omega_a \gg \lambda_i$, we can approximate $\gamma_n(\omega_a + \lambda_i) \approx \gamma_n(\omega_a) = \gamma_n$. Therefore, in principle we do not need to perform the calculation shown in Eq. (15). From an experimental point of view we have chosen the relaxation time equal to $\tau_{cav} = \tau_{fib} = 0.1\ \mu$s, or γ_1=γ_2=γ_3=10 MHz.

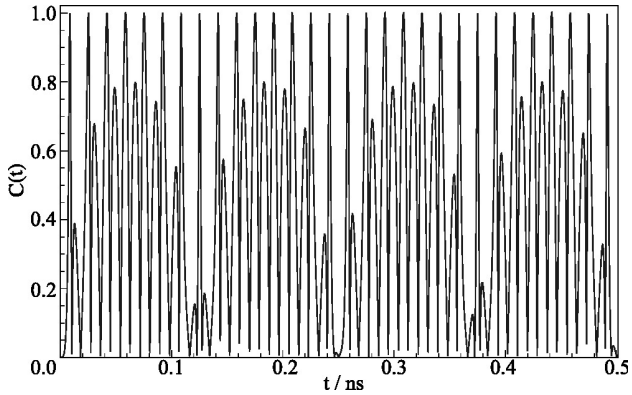

FIGURE 2. Concurrence in the absence of atom-cavity detuning and losses. The coupling constants are $g_1 = g_2 = \nu = 2\pi \times 30$ GHz. The figure shows central peaks with maximum concurrence, and intermediate oscillations with smaller amplitudes.

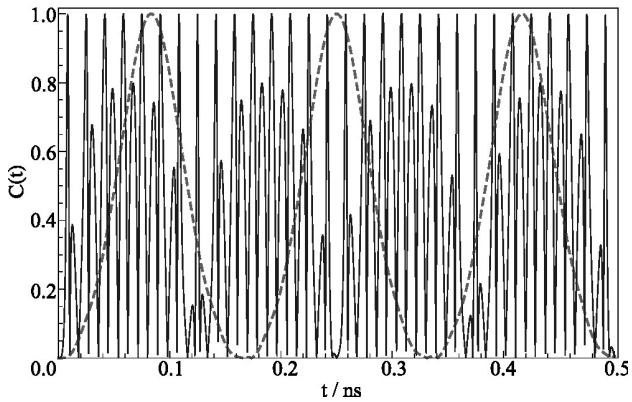

FIGURE 3. The graph compares the generation of atomic entanglement for two different sets of parameters. First, we consider $g_1 = g_2 = \nu = 2\pi \times 30$ GHz (solid line) (see Fig. 2). In the second case, we have $g_1 = g_2 = 2\pi \times 3$ GHz, and $\nu = 2\pi \times 30$ GHz (dashed line). In both cases, we did not consider losses nor atom-cavity detuning. We notice that, in the dashed line the intermediate oscillations have been reduced and the width of the central peaks are enhanced.

Note that this values and the regime used in our model is within the reach of current technology [23].

On the other hand, the atoms have a long radiative lifetime, which makes atomic relaxations negligible during the interactions of the atoms with the cavities.

We begin the analysis considering a wavelength of 852 nm for the transition of our two-level atoms [31], and equal coupling constants $g_1 = g_2 = \nu = 2\pi \times 30$ GHz. Without atom-cavity detuning, and in the absence of losses.

In this first case, we can observe strong oscillations in the concurrence, between 0 and 1, as well as intermediate oscillations with smaller amplitudes (see Fig. 2). These oscillations have been observed also in other models [16] when two distant atoms are located inside a single-mode optical cavity, even though in Ref. 16 there is only one cavity, the dynamics is similar, *i.e.*, identical atoms interacting with one cavity

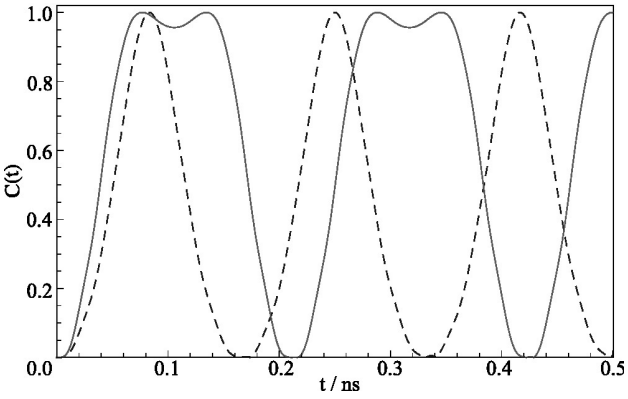

FIGURE 4. Concurrence is generated in the shape of several time-plateau. In solid line corresponds to unequal coupling constants $g_1 = 2\pi \times 3$ GHz, $g_2 = 2\pi \times 6$ GHz, and $\nu = 2\pi \times 30$ GHz. The dashed line, corresponds to $g_1 = g_2 = 2\pi \times 3$ GHz, and $\nu = 2\pi \times 30$ GHz (see Fig. 3). There is no dissipation nor detuning.

mode, the atoms are distant and the coupling strength with the mode are sensitive to the position of the atom inside the cavity, therefore, it produces a feedback of the interactions between the atom and fields, however in our case we can generate entanglement between distant atoms and also between distant cavities.

We can reduce the intermediate oscillations taking $g_1, g_2 < \nu$, and also increase the width of the central peaks (see Fig. 2), as we can see in Fig. 3. A similar dynamic has been observed by Ogden *et al*. [32], even though they do not consider the quantized fibre mode nor losses. In that case, they have two identical cavities, each contains a two-level atom, and the photons are able to hop between the cavities. We also observed that in the regime given by $g_1, g_2 > \nu$, no improvement was achieved.

If we considered unequal coupling constants for the atom-cavity and cavity-fiber interaction, *i.e.*, $g_1 = 2\pi \times 3$ GHz, $g_2 = 2\pi \times 6$ GHz, and $\nu = 2\pi \times 30$ GHz, a small plateau is generated in the time domain, as we see in Fig. 4.

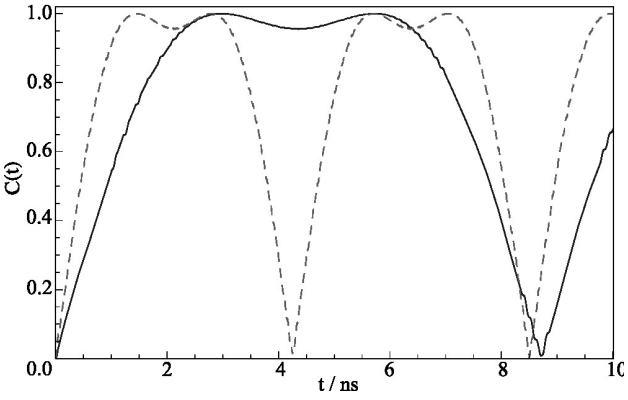

FIGURE 5. Both curves have $g_1 = 2\pi \times 3$ GHz, $g_2 = 2\pi \times 6$ GHz, and $\nu = 2\pi \times 30$ GHz (without losses). However, we have included an atom-cavity detuning of $\Delta = 2\pi \times 100$ GHz (dashed line), and $\Delta = 2\pi \times 200$ GHz (solid line). In the last case, there is a plateau approximately of 4ns wide.

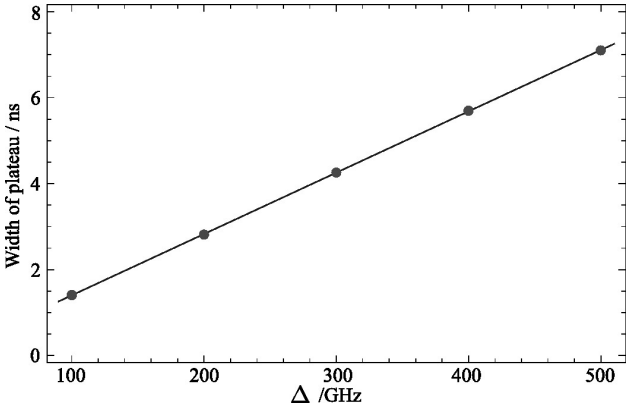

FIGURE 6. The graph shows the dependence of the plateau in the concurrence, versus the atom-cavity detuning (Δ). We observe a linear increase in the range of 100 GHz $\leq \Delta/2\pi \leq$ 500 GHz. The parameters are $g_1 = 2\pi \times 3$ GHz, $g_2 = 2\pi \times 6$ GHz, and $\nu = 2\pi \times 30$ GHz, $\gamma_1 = \gamma_2 = \gamma_3 = 10$ MHz.

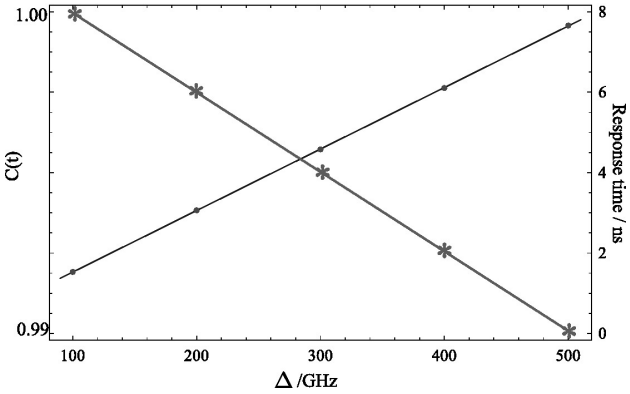

FIGURE 7. The graph shows the dependence of the maximum concurrence, versus atom-cavity detuning (Left axis ($*$)). Also, we show the response time of the system to reach this maximum (Right axis ($\bullet$)). We have set $g_1 = 2\pi \times 3$ GHz, $g_2 = 2\pi \times 6$ GHz, $\nu = 2\pi \times 30$ GHz, and the relaxation frequencies $\gamma_1 = \gamma_2 = \gamma_3 = 10$ MHz.

In order to improve the width of the plateau generated above, we have included a small atom-cavity detuning (as compared with the transition frequency of the atom), taking the value $\Delta = \omega_c - \omega_a = 100$ GHz. We observe an impressive increase of the width of the plateau (see Fig. 5).

In order to study a more complex and realistic case, we now include the decay parameters described in the beginning of this section. *i.e.*, $\gamma_1 = \gamma_2 = 1/\tau_{cav} =$, and $\gamma_3 = 1/\tau_{fib}$.

Next, we study the dependence of the width of concurrence plateau with the atom-cavity detuning. We observe a linear dependence of the width of the plateau with the detuning, as we see in Fig. 6.

When losses are included in the model, the maximum concurrence decreases and the response time of the system (time required to reach the maximum) increases with the detuning (Fig. 7).

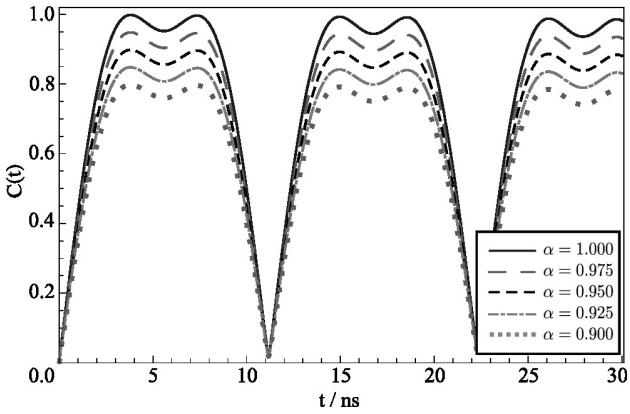

FIGURE 8. Concurrence as function of time for different initial conditions. We consider $\hat{\rho}(0) = \alpha\,|eg000\rangle\langle eg000| + (1-\alpha)\,|ge000\rangle\langle ge000|$. We took the following parameters, $\gamma_1 = \gamma_2 = \gamma_3 = 10$ MHz, $g_1 = 2\pi \times 3$ GHz, $g_2 = 2\pi \times 6$ GHz, $\nu = 2\pi \times 30$ GHz, and $\Delta = 2\pi \times 300$ GHz. As we decrease α, we observe the same behaviour of the system, with a slightly reduced concurrence.

Finally, we show that our system is robust to small variations of the initial state (*i.e.*, the concurrence remained with the same shape, with a small decrease).

As we have seen in Sec. 4-b, we have defined the initial state as:

$$\hat{\rho}(0) = \alpha\,|eg000\rangle\langle eg000| + (1-\alpha)\,|ge000\rangle\langle ge000|\,,$$

with the variable parameter α. For example, for $\alpha = 1$, we have a separable pure initial state. On the other hand, for $0 \leq \alpha \leq 1$, we have initial separable mixed states (see Fig. 8).

6. Conclusions

We have generated atomic entanglement using two two-level atoms, each one inside (trapped) in an optical cavity, the two cavities being coupled by an optical fiber.

We considered the short-fiber limit (It is the only assumption made in the optical fiber), this approximation considers essentially only one (resonant) mode of the fiber interacting with the cavity modes. An open problem not addressed here, might be to consider a long fiber with a phase propagation factor. Also, we neglected the losses due to spontaneous emission of the atoms. However, we considered the cavity losses and the dissipation in the optical fiber. We model the losses using the microscopic master equation at zero temperature. This approach considers quantum jumps between the dressed-states of the full Hamiltonian of the system $\hat{H}_s$.

In the general case, we have took γ_1=γ_2=γ_3=10 MHz, corresponding to the relaxation time for cavities, and optical fiber, respectively.

We generated a major time-plateau in the concurrence, using different coupling constants $g_1 = 2\pi \times 3$ GHz, $g_2 = 2\pi \times 6$ GHz, $\nu = 2\pi \times 30$ GHz, getting further improvement when a small atom-cavity detuning was present.

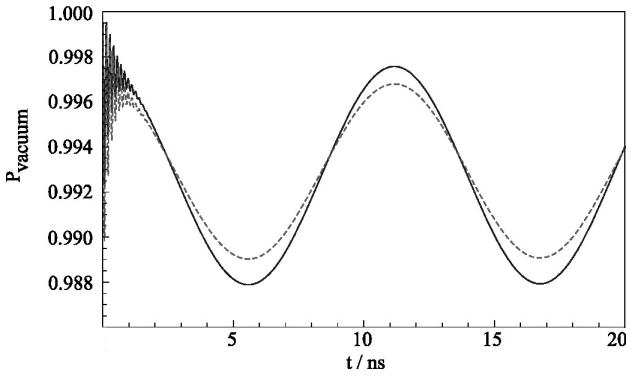

FIGURE 9. The graph shows the probability of have simultaneously the vacuum state for cavities and the optical fiber, for $\alpha = 0.9$ (dashed line), and $\alpha = 1.0$ (solid line), $\gamma_1 = \gamma_2 = \gamma_3 = 10$ MHz, $g_1 = 2\pi \times 3$ GHz, $g_2 = 2\pi \times 6$ GHz, $\nu = 2\pi \times 30$ GHz, and $\Delta = 2\pi \times 300$ GHz. As we can see, there is a high probability of obtaining the simultaneous vacuum states.

In presence of losses, the system shows a linear increase in the plateau, versus the atom-cavity detuning.

On the other hand, the system shows a linear decrease of the concurrence, as well as, an increase in the response time of the system versus detuning.

Furthermore, the system is robust to small variations of the initial state.

From an experimental point of view, in our particular situation, we need distinguish a single-photon state from zero-, and one-photon states. In order to accomplish the measurement, we pass an atom (or a flux of atoms) in its ground state through the cavities. If the cavity was initially in zero-photon state, nothing will happen to the atom, however, if we measure the auxiliary atom in the excited state, we can conclude that the cavity must have been in a single photon state [14].

On the other hand, to show the efficiency of such simultaneous measurement, we can calculate the probability of this happening as follows:

$$\hat{\rho}_{fields}(t) = \sum_{i,j} \langle\phi_i|\,\hat{\rho}(t)\,|\phi_j\rangle\,(\langle eg|\phi_i\rangle\langle\phi_j|eg\rangle + \langle ge|\phi_i\rangle\langle\phi_j|ge\rangle + \langle gg|\phi_i\rangle\langle\phi_j|gg\rangle), \qquad (16)$$

where we have traced the Eq. (13) in the atomic base $\{|eg\rangle\,,|ge\rangle\,,|gg\rangle\}$. In the Eq. (16), the density matrix $\hat{\rho}_{fields}(t)$ is written in the base $\{|000\rangle\,,|001\rangle\,,|010\rangle\,,|100\rangle\}$. Therefore, the probability of measuring simultaneously the vacuum state corresponds to the normalized matrix element $\langle 000|\,\hat{\rho}_{fields}(t)\,|000\rangle$.

As we can see in the Fig. 9, there is a high probability of that our system is in the simultaneous vacuum state for both cavities and the optical fiber.

Acknowledgments

M.O was supported by Fondecyt # 1100039.

1. A. Acín, T. Durt, N. Gisin, and J.I. Latorre, *Phys. Rev. A* **65** (2002) 052325.
2. A. Acín, R. Gill, and N. Gisin, *Phys. Rev. Lett.* **95** (2005) 210402.
3. Yeong-Cherng Liang and A.C. Doherty, *Phys. Rev. A* **75** (2007) 042103.
4. S. Popescu, *Phys. Rev. Lett.* **74** (1995) 2619.
5. R.F. Werner, *Phys. Rev. A* **40** (1989) 4277.
6. A. Einstein, B. Podolsky, and N. Rosen, *Phys. Rev.* **47** (1935) 777.
7. E.T. Jaynes and F.W. Cummings, *IEEE* **51** (1963) 89.
8. M. Orszag, *Quantum Optics*, (2nd ed, Springer Verlag, Berlin, 2007)
9. H. Walther, B.T.H. Varcoe, B.-G. Englert, and T. Becker, *Rep. Prog. Phys.* **69** (2006) 1325.
10. J.M. Raimond, M. Brune, and S. Haroche, *Rev. Mod. Phys.* **73** (2001) 565.
11. X. Maître *et al.*, *Phys. Rev. Lett.* **79** (1997) 769.
12. M. Brune *et al.*, *Phys. Rev. Lett.* **76** (1996) 1800.
13. S. Kuhr *et al.*, *App. Phys. Lett.* **90** (2007) 164101.
14. C,D. Ogden, M. Paternostro, and M.S. Kim, *Phys. Rev. A* **75** (2007) 042325.
15. D.E. Browne, M.B. Plenio, and S.F. Huelga, *Phys. Rev. Lett.* **91** (2003) 067901.
16. S. Natali and Z. Ficek, *Phys. Rev. A* **75** (2007) 042307.
17. T. Pellizzari, *Phys. Rev. Lett.* **79** (1997) 5242.
18. Z.R. Zhong, *Opt. Commun.* **283** (2010) 1972.
19. B.F.C. Yabu.Uti, F.K. Nohama, and J.A. Roversi, *International Journal of Quantum Information (IJQI)* **06** (2008) 1021.
20. Z.Q. Yin and F.L. Li, *Phys. Rev. A* **75** (2007) 012324.
21. D.G. Angelakis, L. Dai, and L.C. Kwek, *EPL* **91** (2010) 10003
22. Lim Yuan Liang, S.D. Barret, A, Beige, P. Kok, and L.C. Kwek, *Phys. Rev. A* **73** (2006) 012304
23. A. Serafini, S. Mancini, and S. Bose, *Phys. Rev. Lett.* **96** (2006) 010503.
24. M. Wilczewski and M. Czachor, *Phys. Rev. A* **79** (2009) 033836.
25. M. Scala, B. Militello, A. Messina, J. Piilo, and S. Maniscalco, *Phys. Rev. A* **75** (2007) 013811.
26. E.B. Davies, *Comm. Math. Phys.* **39** (1974) 91.
27. E.B Davies, *Quantum Theory of Open Systems*, (Academic, London 1976).
28. H.P. Breuer and F. Petruccione, *The Theory of Open Quantum Systems*, (Clarendon, Oxford 2006).
29. W.K. Wootters, *Phys. Rev. Lett.* **80** (1998) 2245.
30. M. Orszag and M. Hernandez, *Adv. Opt. Photon.* **2** (2010) 229.
31. S.M. Spillane *et al.*, *Phys. Rev. A* **71** (2005) 013817.
32. C.D. Ogden, E.K. Irish, and M.S. Kim, *Phys. Rev. A* **78** (2008) 063805.